Soil Biology and Biochemistry 163 (2021) 108446

Contents lists available at ScienceDirect

Soil Biology and Biochemistry

journal homepage: www.elsevier.com/locate/soilbio

A coupled function of biochar as geobattery and geoconductor leads to stimulation of microbial Fe(III) reduction and methanogenesis in a paddy soil enrichment culture

Zhen Yang [a,b], Tianran Sun [c], Sara Kleindienst [d], Daniel Straub [d,e], Ruben Kretzschmar [f], Largus T. Angenent [c], Andreas Kappler [a,g,*]

[a] Geomicrobiology, Center for Applied Geoscience, Tuebingen, 72076, Germany
[b] College of Urban and Environmental Science, Peking University, Beijing, 100871, China
[c] Environmental Biotechnology, Center for Applied Geoscience, Tuebingen, 72076, Germany
[d] Microbial Ecology, Center for Applied Geoscience, Tuebingen, 72076, Germany
[e] Quantitative Biology Center (QBiC), Tuebingen, 72076, Germany
[f] Soil Chemistry Group, Institute of Biogeochemistry and Pollutant Dynamics, CHN, ETH, Zurich, 8092, Switzerland
[g] Cluster of Excellence: EXC 2124: Controlling Microbes to Fight Infection, Tuebingen, Germany

ARTICLE INFO

Keywords:
Biochar
Dissimilatory iron reduction
Methanogenesis
Electron transfer pathways
Conductive-particle interspecies electron transfer

ABSTRACT

Biochar can participate in biogeochemical electron transfer processes due to its electron-accepting and donating capabilities (i.e., geobattery) and electron conductivity (i.e., geoconductor). These two functions were separately demonstrated to play a role in biogeochemical iron cycling and methane formation. Yet, little is known about the coupled effect of both electron transfer mechanisms, even though naturally occurring electron transfer through biochar is expected to simultaneously rely on both geobattery and geoconductor mechanisms. Here, we incubated an anoxic paddy soil enrichment culture with acetate as the substrate to investigate how biochar's coupled electron transfer mechanisms influence the electron transfer pathways between microbes and Fe(III) minerals and how it impacts the soil microbial community composition. We found that biochar simultaneously stimulated microbial Fe(III) reduction and methanogenesis by 2.6 and 2.3 fold, but these processes were spatially decoupled. Small biochar particles (5–20 μm) caused higher Fe(III) reduction and methanogenesis rates than large particles (50–100 μm). The addition of biochar enriched a syntrophic acetate-oxidizing co-culture with dominating Fe(III)-reducing *Geobacteraceae* taxa and acetoclastic methanogenic *Methanosarcina* taxa. After acetoclastic methanogenesis stopped, the observed continuing methanogenesis was likely due to interspecies electron transfer caused by biochar functioning as a geoconductor transferring electrons from *Geobacteraceae* to *Methanosarcina*. In summary, the simultaneous occurrence of Fe(III) reduction and methanogenesis leads to the formation of a cell-biochar-mineral battery network and a cell-biochar-cell conductive network in an enrichment culture from a paddy soil.

1. Introduction

Biochar is the pyrolyzed product derived from incomplete combustion of waste biomass under oxygen-limited or -free conditions. Due to its high porosity, nitrogen availability, cation exchange capacity, and high water-holding capacity, biochar is widely used as an organic amendment to improve soil fertility (Lehmann et al., 2011; Sohi et al., 2010). Biochar contains redox-active quinone and hydroquinone functional groups (Keiluweit et al., 2010) and conductive matrices that consist of polyaromatic carbon ring structures (Xu et al., 2013). Electron transfer pathways via biochar include i) electron-accepting and donating cycles through the redox-active functional groups, meaning that biochar can function as a geobattery (Klüpfel and Kleber, 2014; Wu et al., 2017; Sun et al., 2018), and ii) direct electron transfer via the conductive carbon matrices, meaning that biochar can function as a geoconductor (Yu et al., 2015; Sun et al., 2017, 2018). These pathways are responsible for biochar to participate in multiple redox-driven biogeochemical transformations, e.g., enhancing organic contaminant

* Corresponding author. Geomicrobiology, Center for Applied Geosciences, University of Tuebingen, Schnarrenbergstrasse 94-96, D-72076, Tuebingen, Germany.
E-mail address: andreas.kappler@uni-tuebingen.de (A. Kappler).

https://doi.org/10.1016/j.soilbio.2021.108446
Received 24 June 2021; Received in revised form 28 August 2021; Accepted 19 September 2021
Available online 2 October 2021
0038-0717/

degradation (Oh et al., 2012; Yu et al., 2015), mediating microbial ferric iron (Fe(III)) oxyhydroxide or nitrate reduction (Kappler et al., 2014; Xu et al., 2016; Saquing et al., 2016; Prévoteau et al., 2016), and regulating greenhouse gas emissions (Zhou et al., 2017; Yuan et al., 2017). Additionally, the geoconductor function of biochar was suggested to allow electron transfer between microbial cells by serving as a cell-to-cell conduit between electron-donating and electron-accepting microorganisms (Liu et al., 2012; Chen et al., 2014), referenced here as conductive-material interspecies electron transfer (CIET) (Rotaru et al., 2019).

Biochar electron transfer processes modify soil microbial activities and alter microbial community composition (Mukherjee and Lal, 2013; Zhu et al., 2017; Harter et al., 2016; Krause et al., 2018). Particularly, the addition of biochar stimulated microbial anaerobic respiration and accelerated Fe(III) mineral reduction (Zhou et al., 2017), mitigated N_2O emissions by shifting the community metabolism toward N_2 production (Hagemann et al., 2017a, 2017b; Harter et al., 2014; Cayuela et al., 2013; Harter et al., 2014, 2014; Woolf et al., 2010), and increased the turnover rate of nitrogen and phosphorus species and their accessibility for microbial growth (DeLuca et al., 2015; Gul and Whalen, 2016). Biochar influences methane (CH_4) production and Fe transformation in rice paddy soils. Methanogens produce CH_4 mainly by accepting electrons that are derived from the degradation of organic matter in paddy soils (Yang and Chang, 1998; Hori et al., 2010; Kögel-Knabner et al., 2010). Meanwhile, microbial Fe(III) reduction represents an alternative electron-accepting process in anoxic paddy soils, which leads to competition for electron sources between methanogens and dissimilatory Fe(III)-reducing bacteria (Lovley and Phillips, 1987; Achtnich et al., 1995; Teh et al., 2008; Friedman et al., 2016; Miller et al., 2015). Biochar is well-known as an electron shuttle (serving solely as a geobattery). It stimulates microbial Fe(III) reduction (Kappler et al., 2014; Xu et al., 2016), with electrons preferentially leading to Fe(III) reduction due to the mitigation of methanogenesis as a response to the application of biochar. The addition of biochar simultaneously increased the rates of both microbial Fe(III) reduction and methanogenesis in an enrichment culture from paddy soils compared to soils without biochar application (Zhou et al., 2017). Previous studies have reported the mitigation of methanogenesis by biochar (Jeffery et al., 2016; Brassard et al., 2016). An increasing number of observations have questioned the geobattery function of biochar-mitigating methanogenesis because of a promotion effect on methanogenesis due to direct interspecies electron transport by biochar functioning as a geoconductor (Zhou et al., 2017).

These two mechanisms were separately demonstrated to play a role in biogeochemical iron cycling and greenhouse gas formation (Zhou et al., 2017; Yuan et al., 2018; Rotaru et al., 2019). A synergistic effect of biochar as geobattery and geoconductor for boosting electron transfer was demonstrated using electrochemical analysis (Sun et al., 2018). Still, these specific synergistic functions of biochar in biogeochemical processes remain unknown. In this case, we here hypothesized that the synergistic effect of wood-derived biochar functioning as geobattery and geoconductor leads to the stimulation of microbial Fe(III) reduction through electron transfer between cells and minerals. Furthermore, wood-derived biochar functioning as a geoconductor can bypass electrons to CH_4 emission from *Geobacteraceae* to *Methanosarcina*. It was previously shown that the amendment of small-particle size biochar and high conductance of biochar led to great extents and rates of microbial Fe(III) reduction and methanogenesis (Yang et al., 2020). In this study, biochar application ratio to Fe mineral content was 1.0 g biochar/mM Fe (III), facilitating aggregation and thus leading to efficient electron transport (Yang et al., 2020). This, in turn, is expected to shift the microbial community composition toward specific syntrophic interactions between Fe(III)-reducers and methanogens via biochar particles, functioning as a geoconductor for electrons into methanogenesis. To verify the coupled function of biochar as a geobattery and geoconductor in Fe (III) reduction, methanogenesis, and its induced microbial responses, we set up incubation experiments with an enrichment culture from a paddy soil with different particle sizes of two wood-derived biochar. This study aims (1) to link the application of biochar to soil microbial community composition change and the abundance of special functional genes for methanogenesis and microbial Fe(III) reduction, including *Geobacter* spp., specific 16S rRNA genes, and methyl-coenzyme M reductase subunit alpha (*mcrA*) genes, (2) to clarify the impacts of the coupled effect of biochar functioning as geobattery and geoconductor on the fate of electrons recovered as CH_4 from methanogenesis or as Fe(II) from microbial Fe(III) (stemming from acetoclastic methanogenesis and CIET), and (3) to evaluate electron bypassing from Fe(III) reduction to methanogenesis mediated by biochar functioning as a geoconductor based on acetate consumption and 2-bromoethanesulfonate (BES) inhibitor experiments.

2. Materials and methods

2.1. Preparation of biochar suspensions

Two biochars, Swiss-biochar (s-biochar, Belmont-sur-Lausanne, VB, Switzerland) from mixed waste wood chips, and KonTiki biochar (k-biochar) from pine wood chips, were used in microcosm incubations. Both biochars were produced by pyrolyzing biomass at 700 °C. The physicochemical properties of biochar are shown in Table S1. As described in the supporting information, the different particle-sized biochar was prepared by milling (Pulverisette, zirconium oxide balls, Fritsch, Idar-Oberstein, Germany). Small-sized (SP) biochar particles have a minor fraction (5%–10% of the volume distribution) of 0.1–0.3 μm and the main fraction (90–95% of the volume distribution) of 5–20 μm and the large-sized (LP) biochar particles are 50–100 μm. As reported previously, anoxic biochar suspensions were prepared (Kappler et al., 2014; Yang et al., 2020).

2.2. Preparation of an anoxic enrichment culture from a paddy soil

Paddy soil was collected from Vercelli, Italy. Detailed information on the soil is provided in Table S2. In the laboratory, 100-g soil was added to a 1000 -mL Schott bottle containing 500 -mL anoxic and sterile doubly-deionized (DDI) water to prepare a soil slurry (in triplicate), which was flushed with N_2 for approximately 1 h and incubated at 28 °C and then overhead shaken at 120 rpm. After three weeks, the enrichment culture was prepared from the three incubated soil slurries (triplicates) by combining the three soil slurries into one batch. The combined enrichment culture without any supplements showed less than 2-mg C/L TOC content. Therefore, the TOC content was too low to serve as an electron shuttle (Jiang and Kappler, 2008).

2.3. Incubation setups

Aliquots (5 mL) of the combined and well-mixed enrichment cultures were added to serum vials (50 mL) containing 20-mL sterilized and anoxic medium. The basal medium (pH 6.8–7.2) contained $MgCl_2{\cdot}6H_2O$ (0.4 g/L), $CaCl_2{\cdot}H_2O$ (0.1 g/L), NH_4Cl (0.027 g/L), and KH_2PO_4 (0.6 g/L), 1-mL/L vitamin solution, 1-mL/L trace element solutions, and 30 mM bicarbonate buffer ($NaHCO_3$). Detailed information on vitamin concentration in the microbial growth medium is provided in Table S3. Acetate (Ace.) (1 mM) and Fe(III) (5 mM as ferrihydrite, Fh) were added as the main electron donor and terminal electron acceptor, respectively, to the reaction vials containing medium with the enrichment cultures. The medium pH was adjusted to 7.0–7.1 using NaOH or HCl (1 M). A redox-active model compound, anthraquinone-2,6-disulfonate (AQDS), as a well-known electron shuttle (Lovley et al., 1996) was used as a control for biochar's function as a geobattery. Furthermore, to evaluate electrons fate from the syntrophic activities of our co-culture with dominant Fe(III)-reducing bacteria and methanogens at low acetate concentration in the presence of biochar, we selectively inhibited the methanogenesis activity by the addition of BES on day 9. Detailed

information on experimental setups is provided in Table S4. In total, nine incubation setups (in triplicates each) were prepared: 1) "No amendment" containing enrichment culture only; 2) "No Fh + s-(k-) biochar" with enrichment culture amended with acetate (1 mM) and small-particle s-biochar (5 g/L) or small-particle k-biochar (5 g/L). 3) "No biochar" with enrichment culture amended with acetate (1 mM) and Fh (5 mM); 4) "Acetate" control with enrichment culture amended with acetate (1 mM) only; 5) "s-(k-) biochar" with enrichment culture amended with acetate, Fh (5 mM), and s-biochar (5 g/L) or k-biochar (5 g/L) with two particle sizes (SP and LP); 6) "s-(k-)biochar-abiotic" with enrichment cultures from gamma-sterilized soil slurries amended with acetate, Fh and s-biochar or k-biochar. 7) "Ferrihydrite" with enrichment culture and Fh (5 mM), 8) "AQDS setups" with enrichment culture amended with acetate (1 mM), Fh (5 mM) and AQDS (100 μM), 9) "BES" with enrichment culture amended with acetate, Fh (5 mM), and biochars plus BES (50 mM). BES was added on day 9. The bottles were incubated at 28 °C without shaking in the dark. The size ranges of biochar particles and Fe(III) concentration used in our experiments are comparable to environmentally relevant biochar particle sizes and Fe concentrations (Jones et al., 2011; Zimmerman and Andrew, 2010; Zhou et al., 2017). A biochar application rate of 125 t/ha and Fh content of 0.013 g Fe(III)/g soil was used in our experiments, which is at the high range of general biochar application rates of 0.5–135 t/ha (Glaser et al., 2002; Bista et al., 2019; Zimmerman and Andrew, 2010; Zhou et al., 2017). Using a high biochar application rate allowed us to accurately determine the kinetically preferred pathway (i.e., electron flow via a geobattery or a geoconductor) in Fe(III) mineral reduction and methane production. All setups were subsampled every two days until day 18. Extractable Fe(II) and Fe(tot), CH_4, and acetate were quantified over time. The pH values were determined and showed ranges of 7.01 ± 0.01 on day 0 and 7.04 ± 0.02 on day 18. A redox-active model compound, anthraquinone-2, 6-disulfonate (AQDS), as a well-known electron shuttle (Lovley et al., 1996), was employed to control biochar's function as a geobattery.

2.4. Analytical techniques

Total Fe(II) (soluble in 1M HCl) and Fe(tot) (soluble in 1M-hydroxylamine hydrochloride, HAHCl) were determined using the ferrozine assay as described by Amstaetter et al. (2012) and Stookey (1970). The CH_4 was detected in the same vials without opening the vials. The proportion of headspace to slurry was 25 mL:25 mL. 200-μL headspace was sampled each time. CH_4 in the headspace was quantified using an SRI 8610C gas chromatograph (SRI Instruments Europe GMBH, Germany) equipped with a flame ionization detector (detection limit 2 ppmv). Liquid samples (ca. 200 μL) for acetate analyses were taken in an anoxic glove box (100% N_2) and filtered through 0.22 μm filters before high-performance liquid chromatography (HPLC, LC-10AT, SHIMADZU) analysis equipped with a DAD and RID detector.

2.5. Bacterial and archaeal 16S rRNA gene amplification, illumina sequencing and data analysis

After 18-days of incubation, soil samples (approximately 3–4 g each) were collected by centrifugation (14,000 g, 30 min), and pellets were kept at −20 °C. According to the manufacturer's protocol, DNA in all treatments was extracted using the Power-SoilTM DNA isolation kit (Mo Bio Laboratories, Carlsbad, CA). The DNA of triplicate samples (i.e., biological replicated) was pooled equally to yield a final concentration of 2 ng/μL for all biotic treatments. To investigate the bacterial and archaeal communities' structure and composition, the V4 regions of universal 16S rRNA genes were amplified using polymerase chain reaction (PCR) with the primer set 515f (5′-GTGCCAGCMGCCGCGGTAA-3′) and 806r (5′-GGACTACHVGGGTWTCTAAT-3′) (Caporaso et al., 2011) using the pooled DNA samples as a template. Amplicons were sequenced using Microsynth AG (Switzerland) with the Miseq platform (Illumina, San Diego, CA, USA) using the v2 chemistry (PE 250), and between 85,557 and 205,129 read pairs were generated for each sample. For each sample, 928–2496 ASVs representing 55,256–150,247 read pairs were finally obtained, and 8957 ASVs were detected across all samples. Sequencing data were analyzed with nf-core/ampliseq v1.1.0 that wraps all analysis steps and software and is publicly available at https://github.com/nf-core/ampliseq (Straub et al., 2020). Briefly, the primers were trimmed, and untrimmed sequences were discarded (<6%) with Cutadapt v1.16 (Martin, 2011). Adapter and primer-free sequences were imported into QIIME2 v2018.06 (Bolyen et al., 2018) quality checked with demux (https://github.com/qiime2/q2-demux), and processed with DADA2 v 1.6.0 (Callahan et al., 2016) to remove PhiX contamination, trim reads before median quality falls below 35 (forward 181, reverse 107), correct errors, merge read pairs and remove PCR chimeras and, ultimately, produce amplicon sequencing variants (ASVs). Alpha rarefaction curves were produced with the QIIME2 diversity alpha-rarefaction plugin, indicating that the richness of the samples was fully observed. A Naive Bayes classifier was fitted with 16S rRNA gene sequences extracted with the PCR primer sequences from SILVA v132 QIIME compatible database clustered at 99% identity (Pruesse et al., 2007) ASVs were classified by taxon using the fitted classifier (https://github.com/qiime2/q2-feature-classifier). 43 ASVs classified as chloroplast or mitochondria were removed, totaling <0.5% relative abundance per sample and the remaining 8914 ASVs had their abundances extracted by feature-table (Bolyen et al., 2018). The treatments were analyzed at the end of incubation for their microbial community composition.

2.6. Real-time quantitative PCR

The abundances of bacterial 16S rRNA genes, archaeal 16S rRNA genes, *Geobacter* spp. specific 16S rRNA genes and methyl-coenzyme M reductase subunit alpha (mcrA) genes were analyzed using an IQ™5 Multicolor Real-time PCR Detection system (BIO-RAD Laboratories GmbH, München). The reaction mixture contained 3.15 μL DNA (2 ng/μL) as a template for each triplicate, 5-μL SYBR 2 Premix Ex Taq, 0.5 μL each primer, and 3 μL sterilized deionized water. Negative treatment control was conducted using sterilized deionized water instead of a DNA template for each qPCR assay. Detailed information regarding the primers and thermal cycling conditions used is shown in the Supporting Information (Table S4). A 10-fold serial dilution of the standard plasmid DNA was used, and it covered seven orders of magnitude from 10^2 to 10^8 copies of template per test. The standard curves for qPCR are shown in Fig. S5. qPCR was conducted in triplicate, and the final *Geobacteraceae* bacterial 16S rRNA and *mcrA* genes were obtained by calibrating against total DNA concentrations extracted and the volume of anaerobic setups.

2.7. Statistical analysis

Statistical analysis was conducted by the statistics software package SPSS 22.0. Tukey's test determined statistical significance to compare CH_4 emission, Fe(II) production, and acetate consumption, as well as results from qPCR analyses and methanogenesis inhibitor experiments among different setups. Tukey's multiple-comparison test was used to compare 16S rRNA illumina sequencing analysis. Data from the different groups came from populations where the observations have a normal distribution, and the standard deviation is the same for each group. Differences in electron recovery and gene copy numbers of specific functional genes between different biochars particles were verified using a *t*-test. $^{***}P < 0.001$; $^{**}P < 0.01$, $^{*}P < 0.05$, and n.s., not significant.

2.8. Data availability

Raw sequencing data was deposited at the National Center for Biotechnology Information Sequence Read Achives database under BioProject accession number (PRJNA597449).

3. Results

3.1. Rates of Fe(III) reduction and methanogenesis in the presence of biochar

To investigate the biochar effect with small and large particle size on microbial Fe(III) reduction and methane emission in the paddy soil enrichment culture, we monitored Fe(II) concentrations, Fe(II)/Fe(tot) ratios, and CH_4 concentrations for 18 days (Fig. 1A and B). Compared to setups with enrichment culture only ("No amendments" setups, 0.05-mM Fe(II)/d and 5.22 μM CH_4/d), the addition of both Fh and acetate ("No biochar" setups) led to faster Fe(II) formation (0.17-mM Fe(II)/d). Compared to nonamended setups, the setups amended with acetate showed no obvious increase in CH_4 but a significant increase in Fe(II) production (Fig. S7). These results agree with previous studies (Teh et al., 2008; Roden and Wetzel, 2003), suggesting that Fh addition suppressed CH_4 production due to the high thermodynamic favorability (Table S7) of Fh in accepting electrons. When setups were not supplied with Fh as a terminal electron acceptor but amended with biochar and acetate (Fig. 1C, "No Fh + s- (k-)biochar" setups), biochar significantly (Tukey test with $P < 0.001$) stimulated CH_4 production (Fig. 1C) compared to "No amendment" setups. Biochar significantly (Tukey test with $P < 0.001$) stimulated CH_4 production (Fig. 1C) compared to both "Nonamendment" setups and setups amended with acetate only (Fig. S7). Furthermore, the highest extent of increase in CH_4 was observed in setups amended with acetate plus biochar but without Fh ("No Fh + s-(k-) biochar" setups (Fig. 1C). These results indicated that biochar could facilitate electron transfer to methanogenesis in the absence of Fh. Finally, in the setups amended with Fh, acetate, and biochar ("s- (k-) biochar" setups), the addition of biochar simultaneously stimulated both Fe(II) and CH_4 production compared to setups without amended with biochar (Fig. 1A and B, "No biochar" setups, Tukey test with $P < 0.001$). Therefore, adding biochar could stimulate both Fe(II) and CH_4 production, indicating a coupled function of biochar via its geobattery and geoconductor mechanisms.

3.2. The influence of biochar in comparison to AQDS for rates of Fe(III) reduction and methanogenesis

Based on sharply decreased Fe(II) and CH_4 production rates around day 9, we divided the entire incubation duration into two periods (i.e., period 1 for day 1–9 and period 2 for day 10–18). We found that after adding biochar, up to 60% of Fe(II) production was accomplished in period 1 with a high rate of Fe(II) production (0.25–0.37-mM Fe(II)/d, Fig. 1D) than the incubation without biochar ("No biochar" with 0.08 ± 0.01 mM Fe(II)/d, Fig. 1D). Compared with period 1, the Fe(II) production rates were much lower (Fig. 1D) in period 2, especially with biochar amendment. In the absence of biochar, the CH_4 production rate was 1.08-μM CH_4/d in period 1 and increased to 2.27 μM CH_4/d in period 2. AQDS was used to investigate its effect on electron redirection between microbial Fe(III) reduction and methanogenesis compared to biochar. During period 1, the CH_4 production rates in setups amended with AQDS (1.75 μM CH_4/d) were obviously slower than in the biochar-amended setups (10.13–12.80 μM CH_4/d), but similar to the 'no biochar' setup (1.08 μM CH_4/d, Fig. 1D). Additionally, setups amended with AQDS showed a significant stimulation of microbial Fe(III) reduction in period 1 (days 1–9) (0.44 mM Fe(II)/d) compared to setups that did not contain AQDS or biochar (0.08 mM Fe(II)/d). These results indicated that AQDS functioned as a geobattery and only favored microbial Fe(III) mineral reduction but not methanogenesis.

We identified electron fate recovered, as Fe(II) and CH_4 from acetate oxidation in different treatments amended with AQDS or biochar during periods 1 and 2. The rates and extents of acetate oxidation were significantly higher (Tukey test with $P < 0.001$) in setups amended with both small and large particle biochar and in setups with AQDS than in nonamended setups (Fig. 2A and B). In the presence of sufficient acetate (i.e., during incubation period 1), 54%–63% of the added acetate was recovered, as Fe(II) after adding biochars or AQDS, suggesting that biochar had a similar effect as AQDS, and favored microbial Fe(III) mineral reduction. Approximately 6% of acetate was recovered as CH_4 after the amendment of biochar. In contrast, only 1% acetate was recovered as CH_4 after the addition of AQDS (Table S6).

3.3. The impact of biochar type and particle size on rates of microbial Fe (III) reduction and methanogenesis

s-biochar showed higher electron exchange capacity (EEC) and higher conductance values than k-biochar, related to the higher degree of carbonization during the production of this biochar produced from mixed wood compared to biochar produced from other feedstock or low-density wood feedstock (Shen et al., 2018; Werdin et al., 2020). When comparing the two types of biochar, we observed faster rates of Fe(II) and CH_4 production (Tukey test with $P < 0.05$) in setups amended with s-biochar than that with k-biochar (Fig. 1D). This could be due to the higher EEC and higher conductance of s-biochar compared to k-biochar (Table S1). In the case of either s-biochar or k-biochar, we found that small particles (5–20 μm) presented more than 150% and 100% increased rates of Fe(II) (Fig. 1D) and CH_4 production (Fig. 1D) than large biochar particles (50–100 μm), respectively. Furthermore, these increased production rates were probably due to the faster rate of electron transfer (i.e., the Fe(II) production rates) induced by the increased surface area of small biochar particles (1.08% and 1.28% of surface area for s-biochar and k-biochar, respectively, Table S1; Fig. S9) compared to large biochar particle. Furthermore, the higher electron transfer rates (i.e., the higher CH_4 production rates) induced by smaller biochar particles were also related to biochar's higher conductance (Table S1, Fig. 4C).

3.4. The abundance of *Geobacteraceae*, *Methanosarcina* and functional genes related to methane production after addition of biochar

To identify microorganisms that potentially contributed to Fe(III) reduction and methanogenesis in response to biochar addition, we analyzed the microbial community composition and the copy numbers of 16S rRNA genes specific for *Geobacter* spp. and *mcrA* genes (Fig. 3A, S1 and S2). *Geobacteraceae* became the predominant bacterial taxa by accounting for at least 42% of total 16S rRNA gene sequences in the setup without biochar amendment. Two methanogens, *Methanosarcina* and *Methanobacterium*, were detected in all treatments with and without biochar amendment. *Methanosarcina* can metabolize acetate to methane (Li et al., 2018) and also catalyze hydrogenotrophic methanogenesis (Agler et al., 2011). Compared to the setup with only soil ('No amendment' setup), in setups amended with 5 mM Fh and 1 mM acetate ('No biochar' setups) the relative abundance of *Geobacteraceae* increased from 42% to 46%, and *Methanosarcina* increased from 0.2% to 0.4% of 16S rRNA gene sequences, respectively (Fig. 3A). This suggested that Fh and acetate addition increased relative abundance of Fe(III)-reducers affiliating with *Geobacteraceae*. However, no obvious change in the relative abundance of *Methanosarcina* was observed with Fh and acetate amendment. In setups amended with both biochars, the relative abundance of *Geobacteraceae* decreased from 42% to 39% of total 16S rRNA gene sequences (Fig. 3A). However, *Methanosarcina* became the dominant archaeal taxa and accounted for up to 7%–13% of total 16S rRNA gene sequences (Fig. 3A). The relative abundance of *Methanosarcina* of 16S rRNA gene sequences increased by 32-fold in setups amended with biochars compared to setups without biochar amendment. The addition of biochar altered the relative abundance of several other bacterial taxa, including *Rhodocyclaceae*, which decreased in its relative abundance (10%–5%). *Desulfuromonadaceae* and *Syntrophobacterales* increased in relative abundance 3- and 8-fold, respectively, in s- (k-) biochar' setups compared to 'no biochar' and 'no amendment' setups. These results suggest that biochar application enriched dissimilatory Fe(III)-reducing

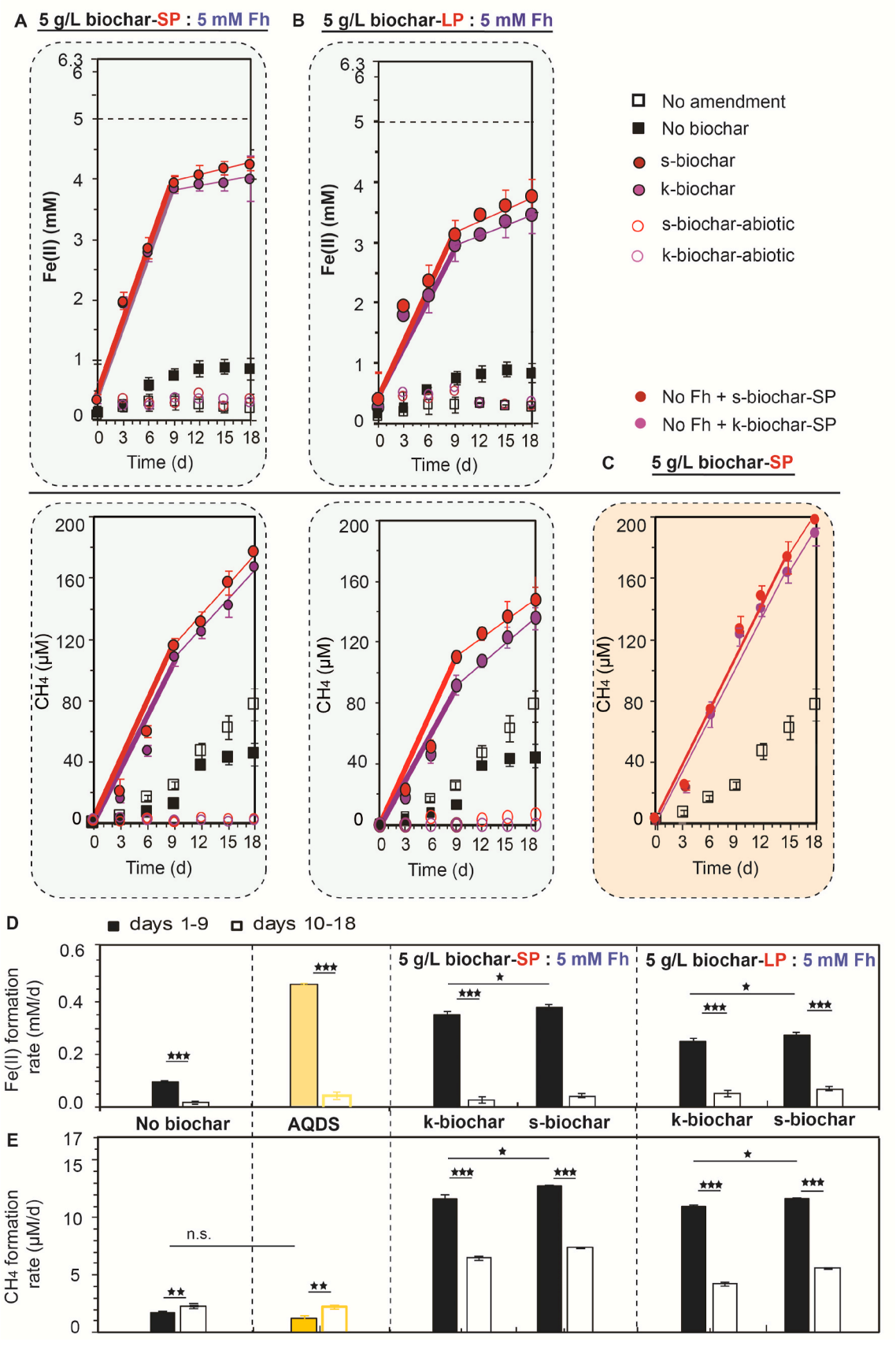

(caption on next page)

Fig. 1. Microbial Fe(III) reduction (upper panel) and methane emission (bottom panel) in anoxic paddy soil enrichment culture amendment with (A) small-particle size (SP) biochar including Swiss biochar (s-biochar, 5 g/L) and KonTiki biochar (k-biochar, 5 g/L), acetate and ferrihydrite (Fh, 5 mM), (B) large-particle size (LP) biochar including s-biochar and k-biochar (5 g/L), acetate and Fh (5 mM). s-/k-biochar-abiotic setups were amended with enrichment culture from the sterilized soil slurry, acetate, Fh, s-biochar or k-biochar, respectively. A close-to-complete microbial Fe(III) reduction resulted in a slow rate of Fe(II) production after day 9. (C) Influence of SP biochars on methanogenesis in setup amended without Fh. The 'No Fh + s- (k-)biochar' setups were amended with acetate, s-biochar-SP or k-biochar-SP, respectively. (D) Rates of microbial Fe(III) reduction (mM Fe(II)/d) and (E) methanogenesis (μM CH_4/d) with biochar-SP/LP and Fh during two incubation periods (period 1: days 1–9 and period 2: days 10–18). The AQDS setup was amended with 100 μM AQDS, 1 mM acetate and 5 mM Fh. Error bars represent standard deviations of triplicate experimental setups. Statistical significance was analyzed by Tukey test. ***P < 0.001; **P < 0.01, *P < 0.05, and n.s., not significant.

bacteria (*Desulfuromonadaceae* and *Syntrophobacterales*), as shown in previous studies (Zhou et al., 2017; Tong et al., 2014).

To further quantitatively assess the role of biochar in modifying soil microbial communities, we used qPCR-specific for 16S rRNA genes of *Geobacter* spp. and for *mcrA* genes. Both genes were detected in all treatments. The copy numbers of *Geobacter* spp. genes and *mcrA* genes both increased after amendment with biochars compared to setups that contained no biochar (Fig. 3B and C, and Fig. S2B and S2C), where we saw no obvious increase in the relative abundance of *Geobacteraceae*. In contrast, the relative abundance of *Methanosarcina* increased on the basis of 16S rRNA gene sequencing (Fig. 3A and Fig. S2). *Methanosarcina* became the dominant methanogen in the presence of biochar accounting for at least 80% abundance of total methanogens based on 16S rRNA sequencing. Additionally, both the copy numbers of *mcrA* genes and the relative abundance of *Methanosarcina* increased for both s-biochar and k-biochar (Fig. 3A and B and Fig. S2), which indicated that the number of *mcrA* genes is attributed to *Methanosarcina* in our study, at least in most part (excluding 20% abundance of *Methanobacterium*). In biochar-amended setups, the copy numbers of 16S rRNA genes of *Geobacter* spp. and *mcrA* genes increased by 4- and 7-fold, respectively, compared to setups without biochar (Fig. S2B). This further highlights the role of *Geobacter*-related Fe(III)-reducers and *mcrA*-carrying methanogenic archaea in the observed Fe(III) reduction and methanogenesis, respectively. Small biochar particles led to higher gene copy numbers of *Geobacter* spp. (*t*-test, $P < 0.05$) and *mcrA* genes (*t*-test, $P < 0.05$) compared to large particle-sized biochar (Fig. S3A). We found a positive correlation between the copy numbers of 16S rRNA genes specific for *Geobacter* spp. and *mcrA* gene (Fig. S3B, $r = 0.98$) for both s-biochar and k-biochar.

3.5. The contribution of electron transfer pathways to methanogenesis

The fate of electrons in syntrophic acetate-oxidizing co-cultures that were recovered as CH_4 during period 1 in setups amended with biochar were quantified. During period 1, 5.0%–6.0% and 6.0%–6.3% of the electrons were recovered as CH_4 in the presence of k-biochar and s-biochar, respectively, which we attribute to acetoclastic methanogenesis and CIET (Figs. 4A and 5D, and Table S5). Approximately 2.0%–3.2% and 2.2%–3.4% of acetate-derived electrons were directly transferred by CIET from *Geobacteraceae* to *Methanosarcina* through conductive s-biochar and k-biochar particles, respectively, recovered as CH_4 (Fig. 5E, Table S5). For both biochars, small particles showed a high electron recovery of CH_4 compared to large particles (Fig. S8, *t*-test with $P < 0.05$). To evaluate the fate of electrons from syntrophic activities of our co-culture with dominating *Geobacteraceae* and *Methanosarcina* during period 2 in the presence of biochar, we selectively inhibited the methanogenesis activity by adding 2-bromoethanesulfonate (BES) on day 9 to the s-(k-) biochar setups (Fig. 4C). We observed that BES addition immediately stopped CH_4 production, as expected (Fig. 4B). However, Fe(II)/Fe(tot) production was unchanged (Fig. 4C), but the copy number of the *Geobacter* spp. gene (days 10–18) increased (*t*-test with $P < 0.05$) (Fig. 3C). This suggested that electron transfer originating from acetate oxidation in period 2 (days 10–18) was controlled by the activity of the Fe(III)-reducers (i.e., *Geobacteraceae*). No significant change in gene copy numbers of *mcrA* were observed during period 2 (Fig. 3B) before and after the addition of BES.

Additionally, we compared copy numbers of the *mcrA* in period 1 (days 1–9) and period 2 (days 10–18) in setups without the addition of BES but amended with biochar. Gene copy numbers of *mcrA* gene showed no significant change between period 2 and period 1. These results indicated that no significant growth of methanogens occurred in period 2, in the presence of biochar; thus the detected CH_4 production after day 9 could not be attributed to acetoclastic and hydrogenotrophic methanogenesis (no H_2 detected). Without BES addition, we observed a significant decrease (Tukey test with $P < 0.01$) in the rate of acetate consumption (from 0.20 ± 0.01-mM per 9-days to 0.08 ± 0.01-mM per 9-days) after day 9 (Fig. 2B and C) when Fe(III) reduction was consistent, implying that acetoclastic methanogenesis would be stopped after day 9 in the presence of biochar. Additionally, 0.2 mM acetate concentration was observed around day 9, suggesting that after this time in the s-(k-) biochar setups (Fig. 2B), CH_4 production by acetoclastic and hydrogenotrophic pathways by acetoclastic methanogens (*Methanosarcina*) stopped due to reaching acetate concentration threshold (0.20 ± 0.01 mM) (Jetten et al., 1990; Westermann et al., 1989). These results suggested that the produced CH_4 after day 9, was likely due to CIET from the *Geobacteraceae* to methanogens via biochar as a geoconductor, due to the thermodynamic threshold of the acetoclastic pathway and no contribution of the hydrogenotrophic pathway since no H_2 was detected over incubation.

4. Discussion

4.1. Simultaneous stimulation of Fe(III) reduction and methanogenesis in the presence of biochar

Stimulation of Fe(III) reduction was observed after amendment with acetate plus biochar and Fh (Fig. 1A). This is similar to previous studies (Kappler et al., 2014; Xu et al., 2016) because of biochar functioning as a geobattery (electron shuttle) facilitating microbial Fe(III) mineral reduction. Compared to nonamended setups, the setup amended with acetate only showed no obvious increase in CH_4 formation but a significant increase in Fe(II) production (Fig S7). Additionally, CH_4 highest increase was observed in setups amended with acetate plus biochar ('No Fh + s-(k-) biochar' setups (Fig. 1C). This suggested that microbial Fe (III) reduction outcompeted methanogenesis in the presence of biochar at high acetate concentrations. When setups were not supplied with Fh as terminal electron acceptor but amended with biochar and acetate (Fig. 1C, 'No Fh + s- (k-) biochar' setups), biochar significantly stimulated CH_4 production (Fig. 1C) compared to 'No amendment' setups, indicating that biochar facilitated electron transfer during methanogenesis in the absence of Fh. Conductive black carbon or carbon cloth involved in CIET processes were shown before stimulating methanogenesis (Rotaru et al., 2018; Li et al., 2018). While conductive carbon (through polyaromatic carbon ring structures in carbon matrices) was shown to stimulate methanogenesis, it was unable to stimulate the transformation of nitrogen compounds or sulfide oxidation, probably due to the lack of redox-active functional groups (Xu et al., 2013). In this study, the addition of biochar (together with acetate and Fh) simultaneously stimulated both rates of Fe(II) and CH_4 production, indicating that a coupled, but spatially separated, function of biochar as geobattery by surface redox-active functional groups and as geoconductor via the polymeric carbon matrix. In contrast to AQDS, which functioned as a geobattery (electron shuttle) and only favored microbial Fe(III) mineral reduction but not methanogenesis, the higher rates and extent of CH_4

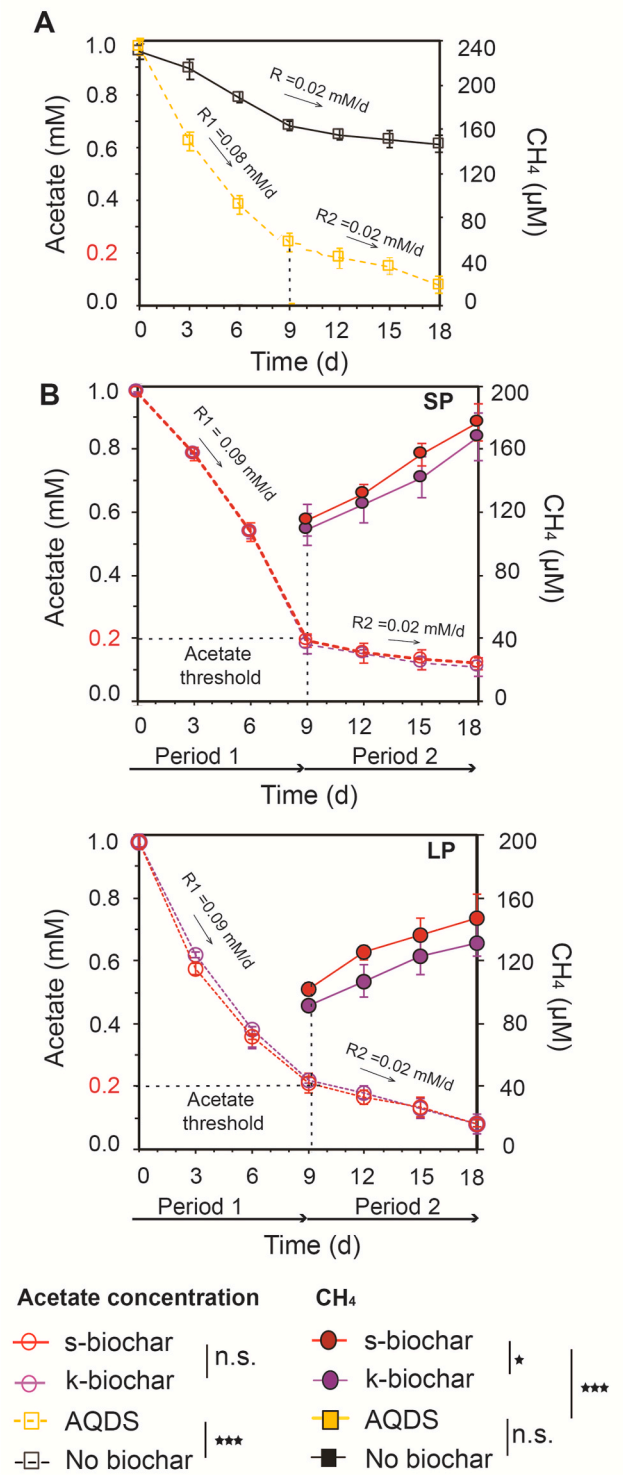

Fig. 2. The relationship of acetate and CH_4 production in different paddy soil enrichment culture setups. (A) "No biochar" setups were amended with enrichment culture, 1 mM acetate and 5 mM Fh. The AQDS setup was amended with enrichment culture, 1 mM acetate, 5 mM Fh and 100 μM AQDS. (B) s-/k-biochar setups were amended with enrichment culture, 1 mM acetate, and s-biochar or k-biochar with small and large-sized particles (SP and LP). The dashed lines indicate it reached the thermodynamic acetate threshold concentration of 0.2 mM that was shown for aceticlastic methanogens such as *Methanosarcina* (Jetten et al., 1990; Westermann et al., 1989). Error bars represent standard deviations of triplicate experimental setups. P values were determined by Tukey test. ***P < 0.001; **P < 0.01, *P < 0.05, and n.s., not significant.

production in the presence of biochar were probably due to biochar geoconductor function, which directly transferred electrons from electron-donating microorganisms to methanogens stimulating CH_4 production.

Furthermore, biochar with the addition of acetate as substrate but without Fh amendment (Fig. S7) showed a positive effect on methanogenesis compared to a non-acetate-amended treatment (Xiao et al., 2019). Promoting growth and immobilization of microorganisms on biochar (Youngwilai et al., 2020) and adsorption of organic matter (e.g., acetate) by biochar (Hill et al., 2019), could also contribute to faster Fe (II) and CH_4 formation in the presence of small biochar particles than large particles. The increased surface area in smaller and higher porosity biochar particles (e.g., carbon fiber and bamboo biochar) can lead to more adhesion of microorganisms to the biochar surface (Jaafar et al., 2015; Afrooz et al., 2018; Liu et al., 2002; Fan et al., 2011). DAX-8 resin porous material that is nonredox-active and nonconductive but has similar porosity and particle size as biochar particles did not influence the electron transfer process (i.e., Fe(II) formation) (Yang et al., 2020). The surface areas of both s- and k-biochar (13–30 m^2 per setup) are 3–6 times larger than ferrihydrite (5 m^2 per setup, Table S1). Biochar is expected to promote the attachment of cells to biochar (Jaafar et al., 2015, Amonette and Joseph, 2009), causing a closer aggregation of cells with biochar compared to only cells with Fh (Yang et al., 2020). This close aggregation can then facilitate direct electron transfer from electron-donating microorganisms to electron-accepting microorganisms through biochar carbon matrices functioning as a geoconductor. The function of biochar as a geoconductor between cells led to a partial bypass of electron flow from cells to Fh. Consequently, electron flow was mediated to methanogens by spatially separated biochar particles, even though Fh is thermodynamically more favorable in accepting electrons (Table S7).

4.2. *The addition of biochar enriched a Co-culture of Geobacteraceae and Methanosarcina*

In biochar-amended enrichment culture setups, the copy numbers of 16S rRNA genes of *Geobacter* spp. and *mcrA* genes increased by 4- and 7-fold, respectively, compared to setups without biochar (Fig. S2B and S2C). This highlights the role of *Geobacter*-related Fe(III)-reducers and *mcrA*-carrying methanogenic archaea for the observed Fe(III) reduction and methanogenesis, respectively, after biochar application. Notably, biochar increased the copy numbers of 16S rRNA genes specific for *Geobacter* spp. and *mcrA* genes. The result indicated that electron transfer from *Geobacteraceae* to *Methanosarcina* through conductive biochar particles leads to CH_4 production in our microcosms, similar as described before (Yuan et al., 2018). Additionally, small biochar particles were more efficient in supporting the growth of *Geobacteraceae* and *Methanosarcina* than large-sized biochar (Fig S8), which could be related to its high surface area because of high acetate adsorption of small particles.

Fe(II) production was not impacted (Fig. 4B) after the addition of BES in period 2 (days 10–18), but both CH_4 production by direct electron transfer via the carbon matrix of biochar and CH_4 production by acetoclastic methanogenesis by *Methanosarcina* were blocked (during period 2) (Fig. 4A). Therefore, electrons stemming from acetate metabolism by *Geobacteraceae* were still transported via biochar functioning as geobattery and geoconductor to stimulate Fe(II) formation. No significant growth of methanogens was detected in period 2 (days 10–18) in the presence of biochar without BES supplement. Additionally, an acetate concentration of 0.2 mM was observed around day 9 suggesting that after this time in the s-(k-) biochar setups (Fig. 2B), CH_4 production by acetoclastic methanogens (*Methanosarcina*) stopped due to reaching the threshold concentration of acetate (0.20 mM) (Jetten et al., 1990; Westermann et al., 1989). The results indicated that the CH_4 produced after day 9 (in period 2, when acetoclastic methanogenesis stopped (Fig. 2B)), was likely a result of CIET from the *Geobacteraceae* to the

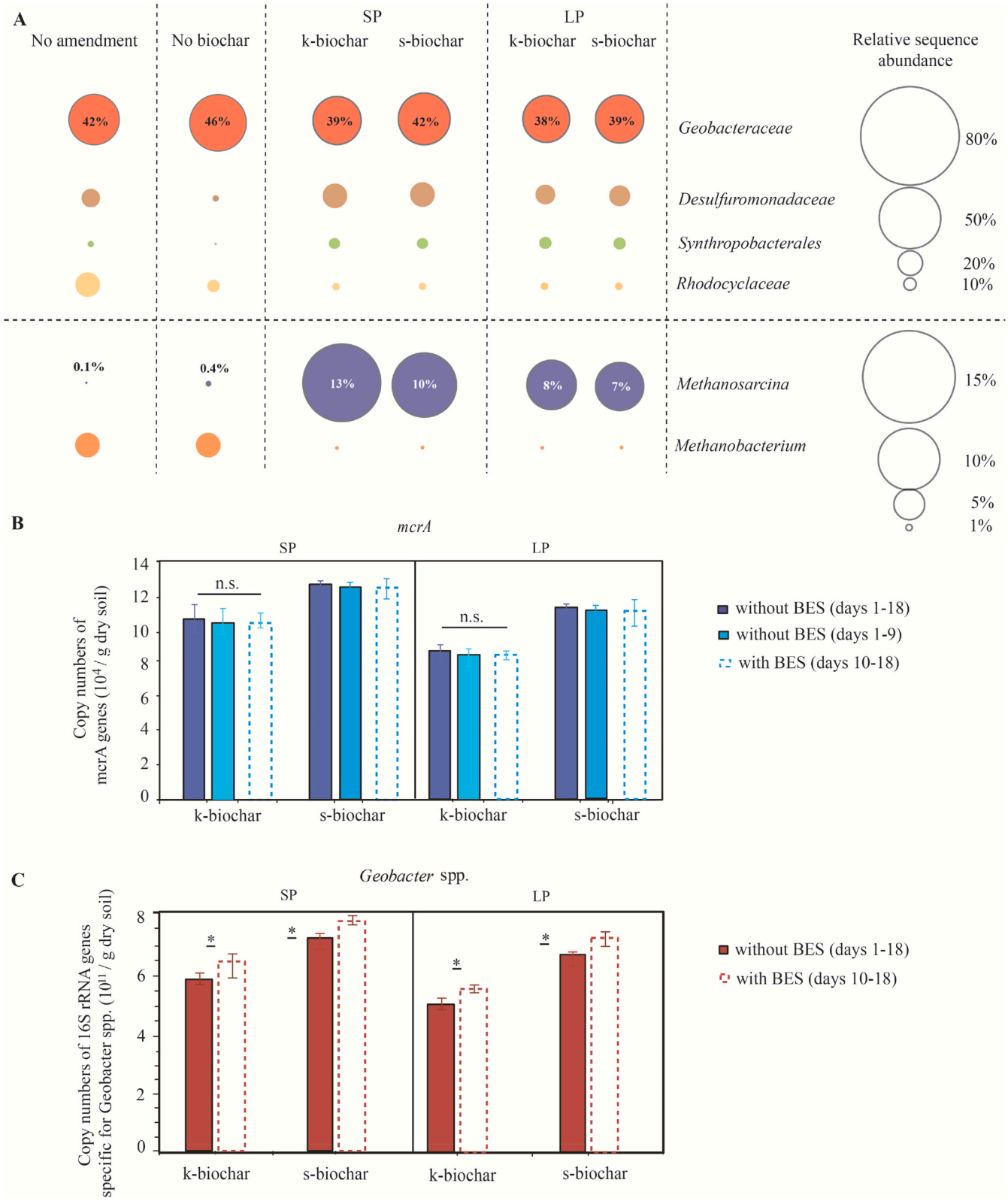

Fig. 3. (A) The relative abundance of *Geobacteraceae* and *Methanosarcina* based on 16S rRNA gene sequencing, respectively, after an 18-day incubation, in setups containing only enrichment culture (no amendments), enrichment culture amended with 1 mM acetate and 5 mM Fh (no biochar) and biochar setups with enrichment culture amended with acetate, Fh and small and large-particle size (SP, LP) Swiss biochar (s-biochar) and KonTiki biochar (k-biochar); (B) Copy numbers of *mcrA* genes and (C) Copy numbers of 16S rRNA genes specific for *Geobacter* spp. per gram dry soil with BES (during days 10–18) and without BES amendment (during days 1–18 and 1–9) in the presence of s- and k-biochar with SP and LP. The BES was added on day 9. Gene copy numbers were quantified on day 9 and 18 respectively. Error bars represent standard deviations of triplicate experimental setups. P values were determined by *t*-test. ***P < 0.001; **P < 0.01, *P < 0.05, and n.s., not significant.

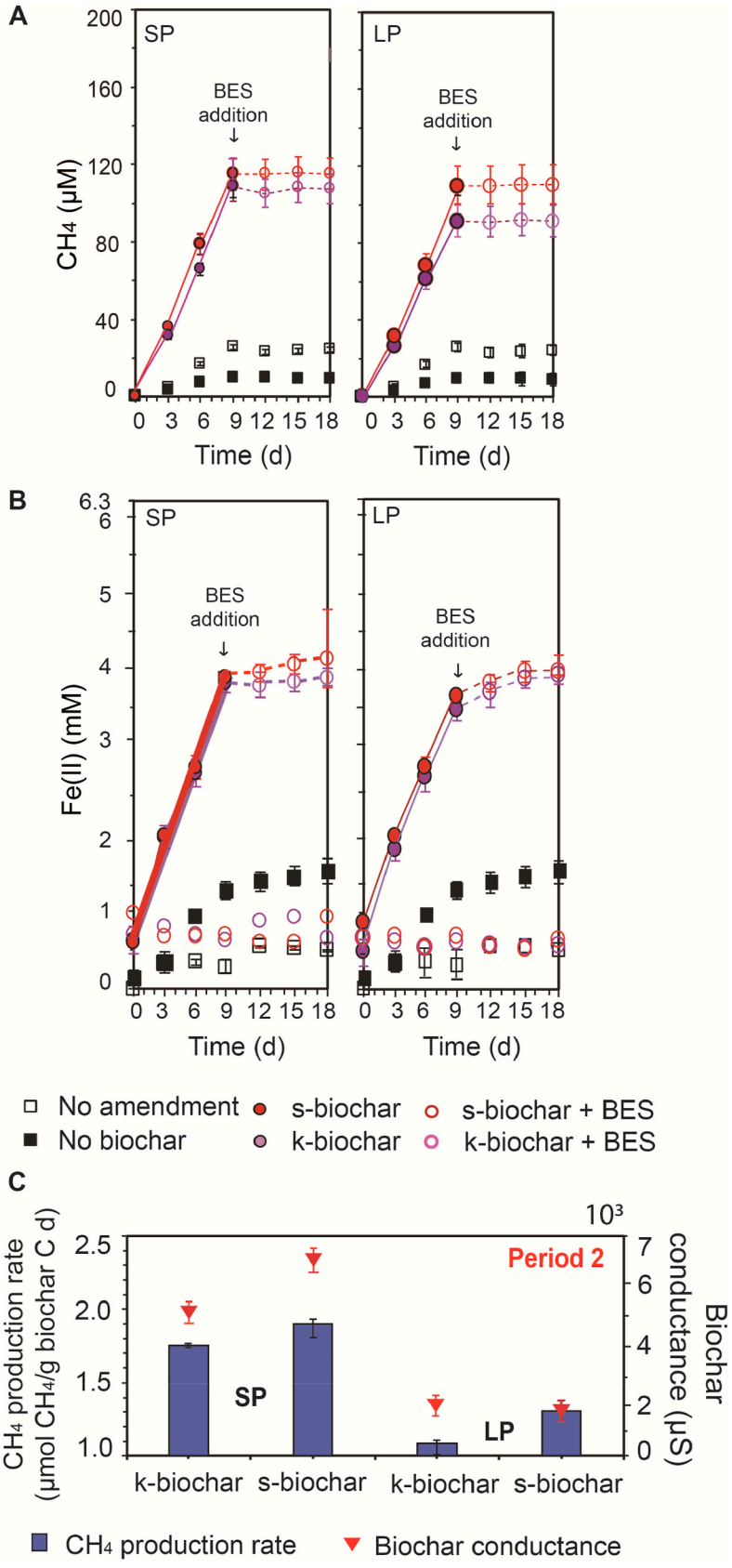

Fig. 4. CH_4 production (A) and microbial Fe(III) reduction (B) in paddy soil enrichment cultures before and after adding a methanogenesis inhibitor (BES, 50 mM). BES was added on day 9. CH_4 production and microbial Fe(III) reduction in paddy soil enrichment culture before and after adding a methanogenesis inhibitor BES (50 mM). BES was added at day 9 in treatments with acetate/ferrihydrite containing either k-biochar or s-biochar with LP and SP compared to setups containing only enrichment culture (no amendment) and enrichment culture amended with 1 mM acetate and 5 mM Fh (no biochar). (C) Relationship between methane formation rates (in μmol CH_4/g (biochar C·d)) in period 2 and conductance of biochar (in μS) in the presence of s-biochar and k-biochar with small and large particles (SP and LP). Error bars represent standard deviations of triplicate experimental setups.

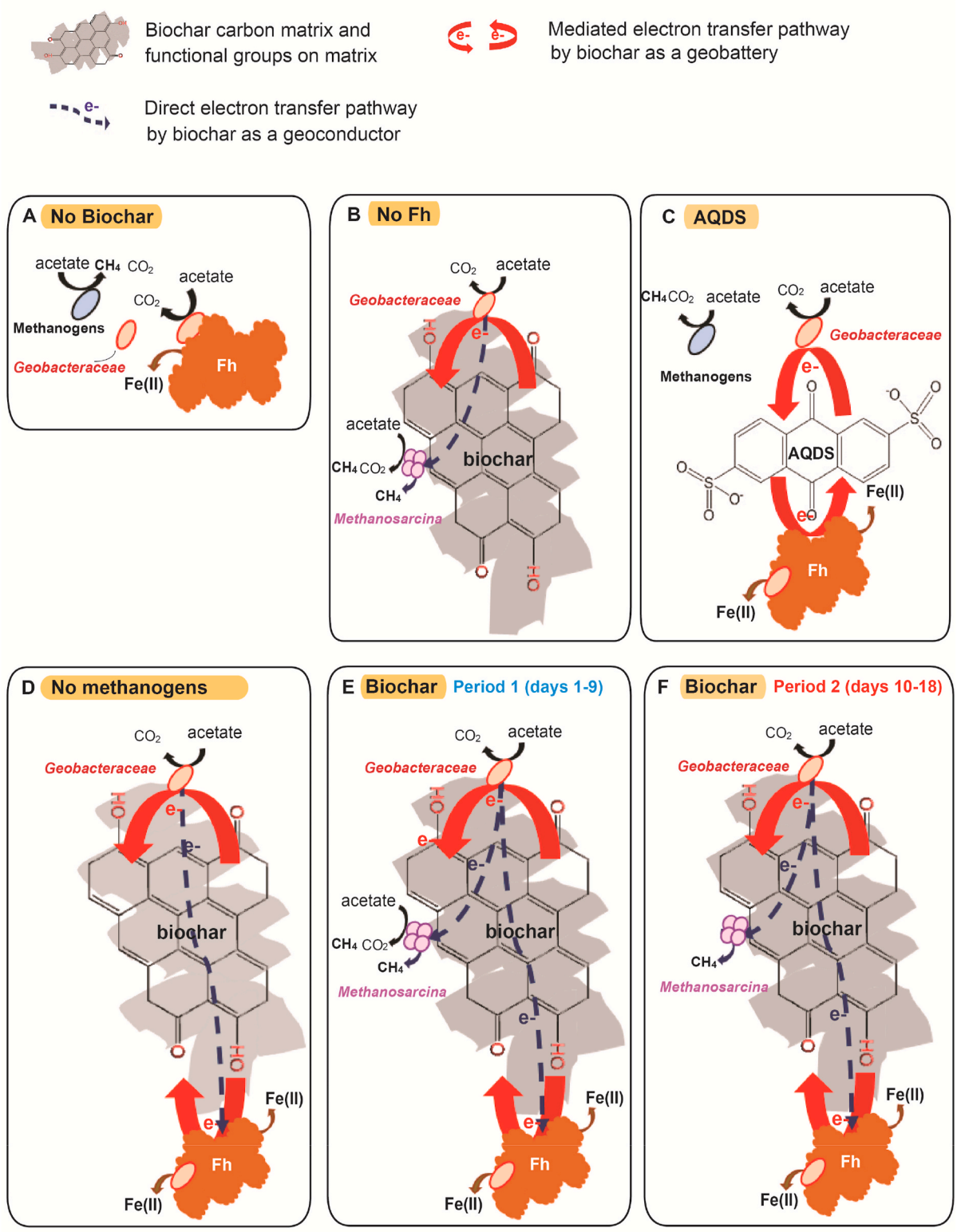

Fig. 5. Schematic of electron transfer pathways between Fe(III)-reducers (*Geobacteraceae*) and methanogens (acetoclastic methanogens or *Methanosarcina*) in anoxic paddy soil enrichment culture setup only amended with (A) acetate and ferrihydrite (Fh) (No biochar), (B) acetate and biochar (No Fh), (C) acetate and AQDS (AQDS), (D) no methanogens, (E) acetate, Fh and biochar during period 1 (biochar setup), and (F) acetate, Fh and biochar during period 2 (biochar setup). Without biochar, microbial Fe(III) reduction outcompetes methanogenesis. Without Fh, biochar contributed to methanogenesis. AQDS as an electron shuttle facilitates electrons transfer between the Fe(III)-reducer and Fh suppressing methanogenesis. Biochar either mediated electron transfer between the Fe(III)-reducer and Fh or directly transferred electrons from the Fe(III)-reducer to the methanogen thus stimulating methane production. Please note that *Geobacteraceae* is the dominating Fe (III)-reducer in our culture and we therefore conclude that microbial Fe(III) reduction is mainly attributed to the metabolism of *Geobacteraceae*. Coupled function of biochar as geobattery and geoconductor, although spatially decoupled, leads to stimulation of microbial Fe(III) reduction and methanogenesis from a paddy soil enrichment.

methanogen via biochar as a geoconductor.

4.3. Altering environmental electron transfer pathways after application of biochar

A comprehensive understanding of the coupled effect of electron transfer mechanisms in biochar (i.e., biochar functioning as geobattery and as geoconductor) was proposed lately from an electrochemical-electron-transfer system using electrochemical analysis (Sun et al., 2017, 2018). We linked the coupled effect of electron transfer mechanism in biochar to the response of microbial metabolism and highlighted biochar's function in simultaneously stimulating CH_4 emission and Fe reduction. Mitigation of CH_4 emission after application of biochar had also been reported in other studies (Feng et al., 2012; Liu et al., 2011; Jeffery et al., 2016; Brassard et al., 2016). This contradictory result to our study could be due to the differences in soil microbial composition (Feng et al., 2012), soil iron contents, and substrate (Harter et al., 2014; Zhou et al., 2017; Zhu et al., 2017; Xiao et al., 2018), and different types of biochar that possess different electron transfer properties (Sun et al., 2017; Klüpfel et al., 2014).

Microbial Fe(III) reduction is thermodynamically more favorable than methanogenesis (Fig. 5A). However, in soils with only low Fe mineral content (Colombo et al., 2014), calcareous soils (Lentz et al., 2014), and Fe(II)/Mn(II)-rich soils in reducing environments (Yu and Patrick, 2004), biochar alternatively functions as a geoconductor and contributes to methanogenesis (Fig. 5B), that means in environments where Fe(III) is depleted as a terminal electron acceptor (Fig. 1C). Diminished methanogenesis occurred in the presence of biochar when microbial Fe(III) reduction became the dominated electron-accepting process (in the presence of sufficient Fe(III)) with biochar functioning as both geobattery and geoconductor). With the input of Fh as Fe(III) source representing Fe-rich paddy soil conditions, the coupled function of biochar as a geobattery and a geoconductor offers dual electron transfer pathways via different biochar particles simultaneously proceed between microbial Fe(III) reduction and methanogenesis. In contrast, the addition of AQDS, which functions only as a geobattery, could only stimulate microbial Fe(III) reduction but did not affect CH_4 emissions (Figs. 1D and 5C). Due to an increasing multidisciplinary application of biochar to soil, water, and sediment (Xie et al., 2015; Rajapaksha et al., 2016; Romero-viana et al., 2011), these electron transfer mechanisms via biochar will occur in some paddy soils, rivers and sediments within Fe-rich habitats containing Fe(III)-reducing bacteria (e.g., *Geobacteraceae*) and methanogenic archaea (e.g., *Methanosarcina*) (Rotaru et al., 2014, 2019; Roden and Wetzel, 2003) in the presence of conductive carbon particles. These environmental locations discussed above are true "hotspots" of significant biogeochemical activities that control element cycles, which impacts the behavior of Fe–Mn mineral phases and metalloids (e.g., As), and nonmetals (e.g., Se). Therefore, CH_4 emission from such environments contributes significantly to the overall greenhouse gas budget on Earth.

Biochar particles easily aggregate with microorganisms in the soil, which induces a fast soil microbial response, particularly of Fe(III)-reducing bacteria and methanogens. In our study, the coupled function of biochar as a geobattery (by electron shuttling) and as a geoconductor, including involved CIET pathway may lead to electron transport either via bacteria-biochar-mineral associations forming a geobattery network or via a bacteria-biochar-archaea conductive network, both potentially relevant for CH_4 emission and Fe(III) reduction. In this context, greenhouse gas regulation and microbial Fe cycling by applying biochar in soil environments need to consider biochar's coupled electron transfer functions as a geobattery and a geoconductor and its induced microbial responses.

Declaration of competing interest

The authors declare that they have no known competing financial interests or personal relationships that could have appeared to influence the work reported in this paper.

Acknowledgements

We gratefully acknowledge support by the China Scholarship Council Foundation (No. 201606510018) for Zhen Yang. Sara Kleindienst is funded by an Emmy-Noether fellowship (grant# 326028733) from the German Research Foundation (Deutsche Forschungsgemeinschaft; DFG). Daniel Straub is funded by the Institutional Strategy of the University of Tübingen (German Research Foundation; DFG, ZUK 63) and further supported by the Collaborative Research Center 1253 CAMPOS (German Research Foundation; DFG, Grant Agreement SFB 1253/1 2017). AK acknowledges infrastructural support by the Deutsche Forschungsgemeinschaft (DFG, German Research Foundation) under Germany's Excellence Strategy, cluster of Excellence EXC2124, project ID 390838134. The authors acknowledge support by the state of Baden-Württemberg through bwHPC and the German Research Foundation (DFG) through grant no INST 37/935-1 FUGG (bwForCluster BinAC). Largus Angenent acknowledges support from the Alexander von Humboldt Foundation in the framework of the Alexander von Humboldt Professorship endowed by the Federal Ministry of Education and Research in Germany. We also thank Ellen Röhm for particle size, TOC/DOC, HPLC analysis, and Joseph G. Usack for methane analysis.

Appendix A. Supplementary data

Supplementary data to this article can be found online at https://doi.org/10.1016/j.soilbio.2021.108446.

References

Achtnich, C., Bak, F., Conrad, R., 1995. Competition for electron donors among nitrate reducers, ferric iron reducers, sulfate reducers, and methanogens in anoxic paddy soil. Biology and Fertility of Soils 19, 65–72.

Afrooz, A.N., Pitol, A.K., Kitt, D., Boehm, A.B., 2018. Role of microbial cell properties on bacterial pathogen and coliphage removal in biochar-modified stormwater biofilters. Environmental Science: Water Research and Technology 4, 2160–2169.

Agler, M.T., Wrenn, B.A., Zinder, S.H., Angenent, L.T., 2011. Waste to bioproduct conversion with undefined mixed cultures: the carboxylate platform. Trends in Biotechnology 29 (2), 70–78.

Amonette, J.E., Joseph, S., 2009. Biochar for environmental management: characteristics of biochar: microchemical properties. In: Lehmann, J., Joseph, S. (Eds.), Biochar for Environmental Management: an Introduction. In Biochar for Environmental Management. Earthscan, London, pp. 33–46.

Amstaetter, K., Borch, T., Kappler, A., 2012. Influence of humic acid imposed changes of ferrihydrite aggregation on microbial Fe(III) reduction. Geochimica et Cosmochimica Acta 85, 326–341.

Bolyen, E., Rideout, J.R., Dillon, M.R., Bokulich, N.A., Abnet, C., Al-Ghalith, G.A., Alexander, H., Alm, E.J., Arumugam, M., Asnicar, F., Bai, Y., 2018. QIIME 2: reproducible, interactive, scalable, and extensible microbiome data science (No. e27295v1). PeerJ Preprints.

Bista, P., Ghimire, R., Machado, S., Pritchett, L., 2019. Biochar effects on soil properties and wheat biomass vary with fertility management. Agronomy 9, 623.

Brassard, P., Godbout, S., Raghavan, V., 2016. Soil biochar amendment as a climate change mitigation tool: key parameters and mechanisms involved. Journal of Environmental Management 181, 484–497.

Callahan, B.J., Mcmurdie, P.J., Rosen, M.J., Han, A.W., Johnson, A.J.A., Holmes, S.P., 2016. DADA2: high-resolution sample inference from Illumina amplicon data. Nature Methods 13, 581. https://doi.org/10.1038/nmeth.3869.

Caporaso, J.G., Lauber, C.L., Walters, W.A., Berg-Lyons, D., Lozupone, C.A., Turnbaugh, P.J., 2011. Global patterns of 16s rrna diversity at a depth of millions of sequences per sample. Proceedings of the National Academy of Sciences of the United States of America 108 (11Suppl. L), 4516–4522.

Cayuela, M.L., Sánchez-Monedero, M.A., Roig, A., Hanley, K., Enders, A., Lehmann, J., 2013. Biochar and denitrification in soils: when, how much and why does biochar reduce N_2O emissions? Scientific Reports 3, 1732.

Chen, S., Rotaru, A.E., Shrestha, P.M., Malvankar, N.S., Liu, F., Fan, W., Lovley, D.R., 2014. Promoting interspecies electron transfer with biochar. Scientific Reports 4, 5019.

Colombo, Palumbo, J.Z., Cesco, P., 2014. Review on iron availability in soil: interaction of fe minerals, plants, and microbes. Journal of Soils and Sediments 14 (3), 538–548.

DeLuca, T.H., Gundale, M.J., MacKenzie, M.D., Jones, D.L., 2015. Biochar effects on soil nutrient transformations. Biochar for Environmental Management: Science, Technology and Implementation 2, 421–454.

Fan, Yuchao, Liu, Wenwen, Youbin, Si, Cui, Hongbiao, 2011. Biodegradation of atrazine in soils by bamboo charcoal immobilized a degradation bacteriu. Soil 43 (6), 954–960.
Feng, Y., Xu, Y., Yu, Y., Xie, Z., Lin, X., 2012. Mechanisms of biochar decreasing methane emission from Chinese paddy soils. Soil Biology and Biochemistry 46, 80–88.
Friedman, E.S., McPhillips, L.E., Werner, J.J., Poole, A.C., Ley, R.E., Walter, M.T., Angenent, L.T., 2016. Methane emission in a specific riparian-zone sediment decreased with bioelectrochemical manipulation and corresponded to the microbial community dynamics. Frontiers in Microbiology 6, 1523.
Glaser, B., Lehmann, J., Zech, W., 2002. Ameliorating physical and chemical properties of highly weathered soils in the tropics with charcoal–a review. Biology and Fertility of Soils 35, 219–230.
Gul, S., Whalen, J.K., 2016. Biochemical cycling of nitrogen and phosphorus in biochar-amended soils. Soil Biology and Biochemistry 103, 1–15.
Hagemann, N., Kammann, C.I., Schmidt, H.P., Kappler, A., Behrens, S., 2017a. Nitrate capture and slow release in biochar amended compost and soil. PLoS One 12, 0171214.
Hagemann, N., Joseph, S., Schmidt, H.P., Kammann, C.I., Harter, J., Borch, T., Kappler, A., 2017b. Organic coating on biochar explains its nutrient retention and stimulation of soil fertility. Nature Communications 8, 1089.
Harter, J., Weigold, P., El-Hadidi, M., Huson, D.H., Kappler, A., Behrens, S., 2016. Soil biochar amendment shapes the composition of N_2O-reducing microbial communities. The Science of the Total Environment 562, 379–390.
Harter, J., Krause, H.M., Schuettler, S., Ruser, R., Fromme, M., Scholten, T., Kappler, A., Behrens, S., 2014. Linking N_2O emissions from biochar-amended soil to the structure and function of the N-cycling microbial community. The ISME Journal 8, 660.
Hill, R.A., Hunt, J., Sanders, E., Tran, M., Burk, G.A., Mlsna, T.E., Fitzkee, N.C., 2019. Effect of biochar on microbial growth: a metabolomics and bacteriological investigation in E. coli. Environmental Science and Technology 53 (5), 2635–2646.
Hori, T., Müller, A., Igarashi, Y., Conrad, R., Friedrich, M.W., 2010. Identification of iron-reducing microorganisms in anoxic rice paddy soil by ^{13}C-acetate probing. The ISME Journal 4, 267.
Jaafar, N.M., Clode, P.L., Abbott, L.K., 2015. Soil microbial responses to biochars varying in particle size, surface and pore properties. Pedosphere 25, 770–780.
Jeffery, S., Verheijen, F.G., Kammann, C., Abalos, D., 2016. Biochar effects on methane emissions from soils: a meta-analysis. Soil Biology and Biochemistry 101, 251–258.
Jetten, M.S., Stams, A.J., Zehnder, A.J., 1990. Acetate threshold values and acetate activating enzymes in methanogenic bacteria. FEMS Microbiology Ecology 6, 339–344.
Jiang, J., Kappler, A., 2008. Kinetics of microbial and chemical reduction of humic substances: implications for electron shuttling. Environmental Science and Technology 42 (10), 3563–3569.
Jones, D.L., Edwards-Jones, G., Murphy, D.V., 2011. Biochar mediated alterations in herbicide breakdown and leaching in soil. Soil Biology and Biochemistry 43 (4), 804–813.
Kappler, A., Wuestner, M.L., Ruecker, A., Harter, J., Halama, M., Behrens, S., 2014. Biochar as an electron shuttle between bacteria and Fe (III) minerals. Environmental Science and Technology Letters 1, 339–344.
Keiluweit, M., Nico, P.S., Johnson, M.G., Kleber, M., 2010. Dynamic molecular structure of plant biomass-derived black carbon (biochar). Environmental Science and Technology 44, 1247–1253.
Krause, H.M., Hueppi, R., Leifeld, J., El-Hadidi, M., Harter, J., Kappler, A., Hartmann, M., Behrens, S., Maeder, P., Hattinger, A., 2018. Biochar affects community composition of nitrous oxide reducers in a field experiment. Soil Biology and Biochemistry 119, 143–151.
Klüpfel, K., Kleber, S., 2014. Redox properties of plant biomass-derived black carbon (biochar). Environmental Science and Technology 48 (10), 5601–5611.
Kögel-Knabner, I., Amelung, W., Cao, Z., Fiedler, S., Frenzel, P., Jahn, R., Schloter, M., 2010. Biogeochemistry of paddy soils. Geoderma 157, 1–14.
Lehmann, J., Rillig, M.C., Thies, J., Masiello, C.A., Hockaday, W.C., Crowley, D., 2011. Biochar effects on soil biota–a review. Soil Biology and Biochemistry 43, 1812–1836.
Lentz, R.D., Ippolito, J.A., Spokas, K.A., 2014. Biochar and manure effects on net nitrogen mineralization and greenhouse gas emissions from calcareous soil under corn. Soil Science Society of America Journal 78 (5), 1641–1655.
Li, J., Xiao, L., Zheng, S., Zhang, Y., Luoc, M., Tong, C., 2018. A new insight into the strategy for methane production affected by conductive carbon cloth in wetland soil: beneficial to acetoclastic methanogenesis instead of co 2 reduction. The Science of the Total Environment 643, 1024–1030.
Liu, F., Rotaru, A.E., Shrestha, P.M., Malvankar, N.S., Nevin, K.P., Lovley, D.R., 2012. Promoting direct interspecies electron transfer with activated carbon. Energy & Environmental Science 5, 8982–8989.
Liu, Y., Yang, M., Wu, Y., Wang, H., Chen, Y., Wu, W., 2011. Reducing CH_4 and CO_2 emissions from waterlogged paddy soil with biochar. Journal of Soils and Sediments 11, 930–939.
Liu, J., He, Z.K., Wang, S.T., 2002. Formation mechanism of carbon fiber biofilms - i. effects of carbon fiber surface characteristics on the immobilization of microorganisms. Xinxing Tan Cailiao/New Carbon Materials 17 (3), 20–24.
Lovley, D.R., Coates, J.D., BluntHarris, E.L., Phillips, E.J.P., Woodward, J.C., 1996. Humic substances as electron acceptors for microbial respiration. Nature 382 (6590), 445–448.
Lovley, D.R., Phillips, E.J., 1987. Competitive mechanisms for inhibition of sulfate reduction and methane production in the zone of ferric iron reduction in sediments. Applied and Environmental Microbiology 53, 2636–2641.
Miller, K.E., Lai, C.T., Friedman, E.S., Angenent, L.T., Lipson, D.A., 2015. Methane suppression by iron and humic acids in soils of the Arctic Coastal Plain. Soil Biology and Biochemistry 83, 176–183.
Mukherjee, A., Lal, R., 2013. Biochar impacts on soil physical properties and greenhouse gas emissions. Agronomy 3, 313–339.
Martin, M., 2011. Cutadapt removes adapter sequences from high-throughput sequencing reads. EMBnet. Journal 17, 10–12.
Oh, S.Y., Son, J.G., Lim, O.T., Chiu, P.C., 2012. The role of black carbon as a catalyst for environmental redox transformation. Environmental Geochemistry and Health 34, 105–113.
Prévoteau, A., Ronsse, F., Cid, I., Boeckx, P., Rabaey, K., 2016. The electron donating capacity of biochar is dramatically underestimated. Scientific Reports 6, 32870.
Pruesse, E., Quast, C., Knittel, K., Fuchs, B.M., Ludwig, W., Peplies, J., Glöckner, F.O., 2007. SILVA: a comprehensive online resource for quality checked and aligned ribosomal RNA sequence data compatible with ARB. Nucleic Acids Research 35, 7188–7196.
Rajapaksha, A.U., Chen, S.S., Tsang, D.C.W., Zhang, M., Vithanage, M., Mandal, S., 2016. Engineered/designer biochar for contaminant removal/immobilization from soil and water: potential and implication of biochar modification. Chemosphere 148, 276–291.
Roden, E.E., Wetzel, R.G., 2003. Competition between Fe(III)-reducing and methanogenic bacteria for acetate in iron-rich freshwater sediments. Microbial Ecology 45, 252–258.
Romero-viana, l., julià, R., Schimmel, M., Camacho, A., Vicente, E., Miracle, M.R., 2011. Reconstruction of annual winter rainfall since a.d. 1579 in central-eastern Spain based on calcite laminated sediment from lake la cruz. Climate Change 107, 343–361.
Rotaru, A.E., Shrestha, P.M., Liu, F., Markovaite, B., Chen, S., Nevin, K.P., Lovley, D.R., 2014. Direct interspecies electron transfer between *Geobacter metallireducens* and Methanosarcina barkeri. Applied and Environmental Microbiology 80, 4599–4605.
Rotaru, A.E., Calabrese, A.F., Stryhanyuk, B.H., Musat, B.F., Shrestha, B.P.M., 2018. Conductive particles enable syntrophic acetate oxidation between *Geobacter* and *Methanosarcina* from coastal sediments. mBio 9 (3) e00226-18.
Rotaru, A.E., Posth, N.R., Löscher, Carolin R., Miracle, M.R., Thamdrup, B., 2019. Interspecies interactions mediated by conductive minerals in the sediments of the iron rich meromictic lake la cruz, Spain. Limnética 38 (1), 21–40.
Saquing, J.M., Yu, Y.H., Chiu, P.C., 2016. Wood-derived black carbon (biochar) as a microbial electron donor and acceptor. Environmental Science and Technology Letters 5, b00354.
Shen, Z., Zhang, Y., Jin, F., 2018. Comparison of nickel adsorption on biochars produced from mixed softwood and *Miscanthus* straw. Environmental Science and Pollution Research 25, 14626–1463.
Sun, T., Levin, B.D., Guzman, J.J., Enders, A., Muller, D.A., Angenent, L.T., Lehmann, J., 2017. Rapid electron transfer by the carbon matrix in natural pyrogenic carbon. Nature Communications 8, 14873.
Sun, T., Levin, B.D., Schmidt, M.P., Guzman, J.J., Enders, A., Martínez, C.E., Muller, D. A., Angenent, L.T., Lehmann, J., 2018. Simultaneous quantification of electron transfer by carbon matrices and functional groups in pyrogenic carbon. Environmental Science and Technology 52, 8538–8547.
Straub, D., Blackwell, N., Fuentes, A.L., Peltzer, A., Nahnsen, S., Kleindienst, S., 2020. Interpretations of environmental microbial community studies are biased by the selected 16S rRNA (gene) amplicon sequencing pipeline. Frontiers in Microbiology 11, 550420.
Sohi, S.P., Krull, E., Lopez-Capel, E., Bol, R., 2010. A review of biochar and its use and function in soil. Advances in Agronomy 105 (1), 47–82.
Stookey, L.L., 1970. Ferrozine—a new spectrophotometric reagent for iron. Analytical Chemistry 42, 779–781.
Teh, Y.A., Dubinsky, E.A., Silver, W.L., Carlson, C.M., 2008. Suppression of methanogenesis by dissimilatory Fe (III)-reducing bacteria in tropical rain forest soils: implications for ecosystem methane flux. Global Change Biology 14, 413–422.
Tong, H., Hu, M., Li, F.B., Liu, C.S., Chen, M.J., 2014. Biochar enhances the microbial and chemical transformation of pentachlorophenol in paddy soil. Soil Biology and Biochemistry 70, 142–150.
Werdin, J., Fletcher, T.D., Rayner, J.P., Williams, N.S.G., Farrell, C., 2020. Biochar made from low density wood has greater plant available water than biochar made from high density wood. The Science of the Total Environment 705, 135856.1-135856.8.
Westermann, P., Ahring, B.K., Mah, R.A., 1989. Threshold acetate concentrations for acetate catabolism by aceticlastic methanogenic bacteria. Applied and Environmental Microbiology 55 (2), 1663.
Wu, S., Fang, G., Wang, Y., Zheng, Y., Wang, C., Zhao, F., Zhou, D., 2017. Redox-active oxygen-containing functional groups in activated carbon facilitate microbial reduction of ferrihydrite. Environmental Science and Technology 51, 9709–9717.
Woolf, D., Amonette, J.E., Street-Perrott, F.A., Lehmann, J., Joseph, S., 2010. Sustainable biochar to mitigate global climate change. Nature Communications 1, 56.
Xiao, L., Liu, F., Xu, H., Feng, D., Liu, J., Han, G., 2019. Biochar promotes methane production at high acetate concentrations in anaerobic soils. Environmental Chemistry Letters 17, 1347–1352.
Xiao, L., Liu, F., Liu, J., Li, J., Zhang, Y., Yu, J., Wang, O., 2018. Nano-Fe_3O_4 particles accelerating electromethanogenesis on an hour-long timescale in wetland soil. Environmental Science: Nano 5, 436–445.
Xie, T., Reddy, K.R., Wang, C., Yargicoglu, E., Spokas, K., 2015. Characteristics and applications of biochar for environmental remediation: a review. Critical Reviews in Environmental Science and Technology 45 (9), 939–969.
Xu, W., Pignatello, J.J., Mitch, W.A., 2013. Role of black carbon electrical conductivity in mediating hexahydro-1,3,5-trinitro-1,3,5-triazine (RDX) transformation on carbon surfaces by sulfides. Environmental Science and Technology 47, 7129–7136.
Xu, S., Adhikari, D., Huang, R., Zhang, H., Tang, Y., Roden, E., Yang, Y., 2016. Biochar-facilitated microbial reduction of hematite. Environmental Science and Technology 50, 2389–2395.

Yang, S.S., Chang, H.L., 1998. Effect of environmental conditions on methane production and emission from paddy soil. Agriculture, Ecosystems & Environment 69, 69–80.
Yang, Z., Sun, T., Subdiaga, E., Obst, M., Haderlein, S.B., Maisch, M., Kretzschmar, R., Angenent, L.T., Kappler, A., 2020. Aggregation-dependent Electron Transfer via Redox-Active Biochar Particles Stimulate Microbial Ferrihydrite Reduction. Science of The Total Environment 135515.
Yu, L., Yuan, Y., Tang, J., Wang, Y., Zhou, S., 2015. Biochar as an electron shuttle for reductive dechlorination of pentachlorophenol by *Geobacter sulfurreducens*. Scientific Reports 5, 16221.
Yu, K., Patrick, W.H., 2004. Redox window with minimum global warming potential contribution from rice soils. Soil Science Society of America Journal 68 (6), 2086–2091.
Yuan, Y., Bolan, N., Prévoteau, A., Vithanage, M., Biswas, J.K., Ok, Y.S., Wang, H., 2017. Applications of biochar in redox-mediated reactions. Bioresource Technology 246, 271–281.
Yuan, H.Y., Ding, L.J., Zama, E.F., Liu, P.P., Hozzein, W.N., Zhu, Y.G., 2018. Biochar modulates methanogenesis through electron syntrophy of microorganisms with ethanol as a substrate. Environmental Science and Technology 52, 12198–12207.
Youngwilai, A., Kidkhunthod, P., Jearanaikoon, N., Chaiprapa, J., Supanchaiyamat, N., Hunt, A.J., Ngernyen, Y., Ratpukdi, T., Khan, E., Siripattanakul-Ratpukdi, S., 2020. Simultaneous Manganese Adsorption and Biotransformation by Streptomyces Violarus Strain SBP1 Cell-Immobilized Biochar. Science of The Total Environment 136708.
Zhu, X., Chen, B., Zhu, L., Xing, B., 2017. Effects and mechanisms of biochar-microbe interactions in soil improvement and pollution remediation: a review. Environmental Pollution 227, 98–115.
Zhou, G.W., Yang, X.R., Marshall, C.W., Li, H., Zheng, B.X., Yan, Y., Zhu, Y.G., 2017. Biochar addition increases the rates of dissimilatory iron reduction and methanogenesis in ferrihydrite enrichments. Frontiers in Microbiology 8, 589.
Zimmerman, Andrew, R., 2010. Abiotic and microbial oxidation of laboratory-produced black carbon (biochar). Environmental Science and Technology 44, 1295–1301.